Liquid Crystals
Publication details, including instructions for authors and subscription information:
http://www.informaworld.com/smpp/title~content=t713926090

Solubilization and photoreactivity of *E*-ethyl cinnamate in smectic B mesophases VII. Photoreactions in liquid crystals

J. Stumpe[a]; S. Grande[b]; K. Wolf[a]; G. Hempel[c]
[a] Humboldt University Berlin, Institute of Organic Chemistry, Berlin, Germany [b] Department of Physics, University Leipzig, Leipzig, Germany [c] Department of Physics, Technical University Leuna-Merseburg, Merseburg, Germany

To cite this Article Stumpe, J. , Grande, S. , Wolf, K. and Hempel, G.(1992) 'Solubilization and photoreactivity of *E*-ethyl cinnamate in smectic B mesophases VII. Photoreactions in liquid crystals', Liquid Crystals, 11: 2, 175 — 198
To link to this Article: DOI: 10.1080/02678299208028982
URL: http://dx.doi.org/10.1080/02678299208028982

LIQUID CRYSTALS, 1992, VOL. 11, NO. 2, 175–198

Solubilization and photoreactivity of *E*-ethyl cinnamate in smectic B mesophases

VII. Photoreactions in liquid crystals

by J. STUMPE*†, S. GRANDE‡, K. WOLF†
and G. HEMPEL§

† Humboldt University Berlin, Institute of Organic Chemistry,
Hessische Strasse 1-2, O-1040 Berlin, Germany
‡ University Leipzig, Department of Physics,
Linné Strasse 5, O-7010 Leipzig, Germany
§ Technical University Leuna-Merseburg, Department of Physics,
Otto-Nuschke-Strasse, 0-4200 Merseburg, Germany

(*Received 31 January 1991; accepted 24 September 1991*)

The relative quantum yields of (2+2) photocycloaddition for *E*-ethyl 4-methoxycinnamate **1** have been estimated in smectic and nematic phases as well as in isotropic melts of *trans,trans*-4′-*n*-butyl- and *trans,trans*-4′-ethylbicyclohexyl-4-carbonitrile (CCH-4 and CCH-2). The quantum yield is significantly higher in smectic B phases compared to the values in the isotropic and nematic range. The existence of a second smectic phase, S_2, of CCH-4 has been shown. The photoreaction does not occur in this mesophase. The solubilization behaviour of deuteriated *E*-ethyl 4-methoxycinnamate has been studied by means of ^2H, ^1H, and ^{13}C NMR as well as DSC and thermal microscopy. The cinnamate has a very low solubility in S_B phases (<0·5 wt%) in contrast to the S_2 and nematic phases. The results indicate that phase separation occurs to cinnamate-rich nematic or isotropic regions below the bulk smectic B–nematic transition temperature. Thus, the high quantum yields are due to compartmentalization of the cinnamate in nematic or isotropic spheres of the biphasic smectic B–nematic or smectic B–isotropic systems.

1. Introduction

Recently, much effort has been made towards modifying photochemical reactivity by organized media [1–4, 43]. Thus, quantum yield, product distribution and the stereochemical course of uni and bimolecular photoreactions can be affected by organized media with their specific order and mobility. These two extremes will be realized on the one hand in the high order of crystals with their lack of mobility and conformational flexibility combined with a high rigidity and, on the other hand, in the high mobility of liquids and the lack of long range order. There may be wide variations in combining both properties within diverse mesophases of thermotropic and lyotropic liquid crystals and other self-organizing systems like Langmuir–Blodgett multilayer assemblies, micelles, membranes or microemulsions. As described previously the liquid-crystalline order can exert an effect on Norrish type II photoreaction [5–12], photocycloaddition [13–22], excimer formation [2, 3, 23–26], photo-Fries rearrangement [27], reaction dynamics in excited state [8] and on dynamics of caged radical-pairs [28], unimolecular isomerizations [2, 3, 29] and asymmetric synthesis [2, 3].

* Author for correspondence.

0267–8292/92 $3·00

However, the reasons, its extent and the nature for controlling photochemical reactivity by the liquid-crystalline environment are not clearly understood in detail. At present there are several reasons under discussion, mainly the randomness of molecular motions and conformational flexibility by molecular packing, motional anisotropy, solvent-induced ordering effects, cage and micro-viscosity effects, localization and compartmentalization effects. However, for liquid-crystalline matrices the influence of the ordered state is limited by the mobility, the low degree of order and mesophase specific diffusion anisotropy. Smectic solvents with their rigidity of packing, their higher order and viscosity should show more relevant effects on reactivity [4].

The possibility of the variation of order, packing and dynamics of the identical chemical system only by temperature-dependent self-organization existing in liquid crystals may be used as an interesting tool for mechanistic investigation of photoreactions. The (2 + 2) photocycloaddition of cinnamic acid in the crystalline state is one of the best known photoreactions in the solid state [30, 31]. The reaction is controlled by the crystal lattice (topochemical principle) and may be drastically altered by small changes in geometry. In solution the thermodynamically stable *E*-cinnamic acid derivatives undergo photoisomerization to the *Z* isomer on irradiation. A photostationary state is established between both isomers. The (2 + 2) photocycloaddition occurs as a parallel proceedings reaction to different stereoisomers of truxinic and truxillic acid derivatives. The photodimerization of cinnamic acid derivatives has been investigated in different liquid-crystalline matrices [17–22]. Thus, Weiss suggests a strong preference for head-to-tail cycloaddition in the S_B phase of *n*-butyl stearate by dipole–dipole induced interactions between cinnamate molecules and preorientational effects [21]. Thus, this regioselective cycloaddition should be caused by partially interdigitated, interlayer pairing antiparallel association of cinnamates in the ordered matrix. Recently, we have succeeded in showing that the quantum yield for the (2 + 2) photocycloaddition of rod-like cinnamates is much greater in smectic B phases of polar and non-polar liquid crystals than the values in their nematic phase or the isotropic melt of the same compounds [32].

Trans, trans-4′-alkylbicyclohexyl-4-carbonitriles (CCH-*n*) have been used as highly ordered and optically transparent solvents for spectroscopic [25, 33–35] as well as for photochemical studies [7, 10, 11]. The pure compounds of CCH-4 and CCH-2 have a nematic and a smectic B phase, which is hexagonally ordered for CCH-4 and rhombohedrally ordered for CCH-2 [36, 37]. The guest–host interaction in their smectic B phases has been investigated by NMR methods and by the matrix dependence of the photoreactions [12]. Thus, CCH-4 influences uni and bimolecular photoreactions such as intramolecular triplet quenching [7, 8] and Norrish type II reaction [5, 12] by the restricted conformational mobility of the excited molecules.

The totally saturated hydrocarbon structure of the CCH's causes a small and negative diamagnetic anisotropy. Therefore the director of the nematic and smectic phase is aligned perpendicular to an external magnetic field. The formation of a plastic crystal or cubic mesophase has been postulated in the low temperature region of the S_B

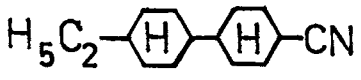

CCH-2
C 29°C S_B 46°C N 49°C I

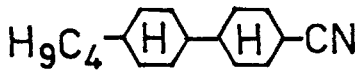

CCH-4
C 28°C S_X 46°C S_B 54°C N 79°C I

phase as a consequence of the temperature depending solubilization of benzene or dioxane [35, 38] as well as alkylphenones [11] in CCH-4 detected by NMR investigations.

It has been shown that aromatic guest molecules have only a small solubility (< 2 mol %) in the smectic B phase of CCH-4 in contrast to a much higher solubility in the nematic phase and the isotropic melt [12]. Recently, a heterogeneous solubility or phase separation has been suggested as the main reason for the surprising spectroscopic and photochemical behaviour of ketones in CCH-4 below the S_B–N transition temperature. Depending on the cooling rate of the guest–host mixture in the S_B region a two phase system was observed. The phase separated system can be a smectic/nematic or smectic/highly concentrated, viscous isotropic biphasic mixture [12].

In the present paper, we report on the guest–host interaction of a deuteriated *E*-ethyl 4-methoxycinnamate in CCH-2 and CCH-4 host matrices by different NMR methods, thermal microscopy and DSC measurements. The matrix dependence of photoisomerization and (2 + 2) photocycloaddition has been correlated with the order and solubilization of the cinnamate in the different mesophases.

2. Experimental section

The optical irradiation was performed with a 500 W high pressure mercury arc lamp combined with a metal-interference filter (313 nm) according to [32]. UV spectra were measured with a UV–VIS spectrometer 'Specord M 40' (VEB Carl Zeiss Jena); potassium ferrioxalate was used as an actinometer. DSC measurements were carried out with equipment from 'HERAEUS'. The DSC thermograms were recorded between −20 and 100°C in heating and cooling cycles, using a 10 K/min temperature programme. In each case air was used as the reference. Transition temperatures and melting points were measured by thermal microscopy.

^{2}H NMR experiments were performed at 13·8 MHz with a home built spectrometer. The temperature was controlled by a regulated air or N_2 stream to ±0·2 K. The spectra were recorded with a 10–15 min waiting period, where thermal equilibrium was established. Spectra were obtained by $\pi/2$ excitation with a pulse length of 3·5 μs. A spectral width of 50 kHz was sufficient for the experiments. 300–1000 scans with a repetition time of 1 s were accumulated and Fourier transformed.

The proton NMR was carried out with $\pi/2$ pulses of 1·5 μs on a Brucker KRS 322 spectrometer at 32 MHz. After 8–32 scans the data were Fourier transformed with a spectral width of 250 kHz. The ^{13}C NMR was measured by means of a cross polarization technique with mixing times of 3 ms and 40 ms acquisition time at 90 MHz in the mesophase and by $\pi/2$ excitation in the isotropic melt. 300 accumulations with a repetition time of 4 s and a spectral width of 10 kHz were used.

The deuteriated *E*-ethyl 4-methoxycinnamate **1** was synthesized using cinnamoyl chloride and deuteriated ethanol [39]. Thus, 4-methoxycinnamic acid and distilled thionyl chloride were mixed. The mixture was heated on a water bath until the HCl and SO_2 were liberated. The 4-methoxycinnamoyl chloride reacts with deuteriated ethanol to give the deuteriated *E*-ethyl 4-methoxycinnamate which was purified by recrystallization twice from ethanol, mp 47–48°C. The structure and the purity of the compound was verified by ^{1}H NMR spectroscopy. The impurities were found to be less than 1 per cent and the deuteriation was higher than 90 per cent of the ethyl group. The guest–host mixtures were prepared by dissolving 0·5, 1·0 and 5·0 wt % of **1** in the isotropic melt of CCH-2 and CCH-4.

The photolyses were carried out in quartz cells with a thickness of 15–20 μm. The carefully cleaned quartz plates were rubbed with velvet attaining a macroscopic surface orientation of the liquid crystals. Mylar foil was used as a spacer between the quartz plates. The liquid crystals were filled into the cell by capillary action in the isotropic melt. These cells were arranged between two black brass blocks with quartz windows situated in a thermostated compartment.

2.1. *Photolysis*

The photochemical behaviour of *E*-ethyl 4-methoxycinnamate **1** is characterized by the competition between *E–Z* photoisomerization and (2+2) photocycloaddition in isotropic melts as well as in the smectic B and nematic mesophases of CCH-2 and CCH-4, as shown in scheme 1. The UV-spectra of the corresponding photolysis of **1** in the smectic B phase as well as in the isotropic melt of CCH-2 is given in figure 1. The competition between *E–Z* photoisomerization and cycloaddition is illustrated in figure 2, where the decreasing absorbance at 313 nm is plotted as a function of the irradiation time. It may be seen that isomerization is faster than cycloaddition in the mesophases and isotropic melts. On irradiation a quasistationary state is established between the geometrical *E* and *Z* isomers and the cycloaddition proceeds as a secondary event. Further irradiation causes the disappearance of the isobestic points as a consequence of cycloaddition. The photoproducts, such as the *E* and *Z* isomer as well as dimeric photoproducts, were detected by FTIR and gas chromatography. The quantum yields of photocycloaddition were estimated by the decreasing absorption at 313 nm as a function of irradiation time, approximating the two photoreactions in a satisfying manner by means of non-linear regression and subsequent extrapolation to zero time. These quantum yields for the (2+2) photocycloaddition of **1** are shown in table 1 and the correlation coefficients of the non-linear regression *r* being better than 0·98 in all cases. An enhancement of quantum yields is observed for this bimolecular reaction in the smectic B phases of CCH-2 and CCH-4 compared to the quantum yield in the isotropic melt and nematic phase of the same solvents.

Thus, the values for the reaction of cinnamate **1** are five times larger in the smectic B phase of CCH-2 and twice to three times larger in CCH-4 compared to that of the isotropic melt. Recently, we have reported a similar behaviour for a number of

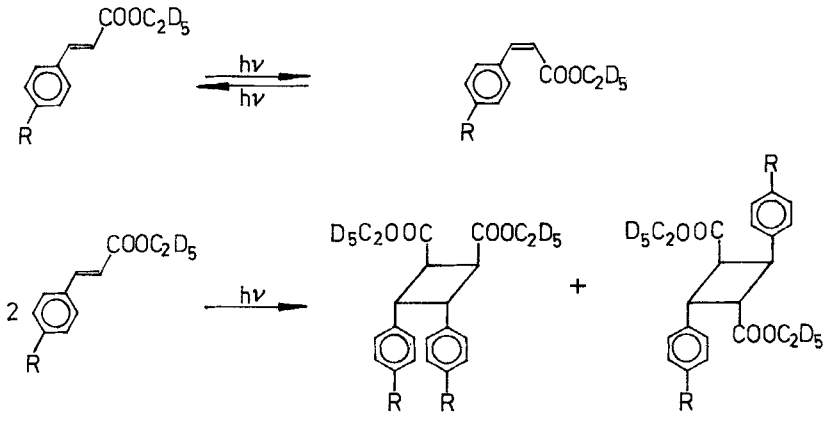

Scheme 1. Photochemical behaviour of cinnamate *E–Z* photoisomerization and (2+2) photocycloaddition.

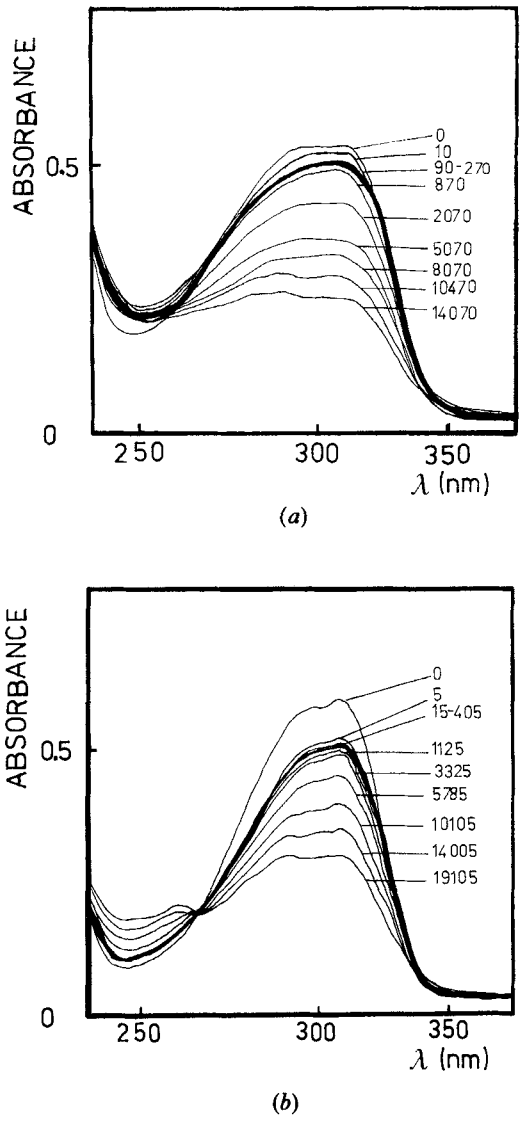

Figure 1. Photolysis of *E*-ethyl 4-methoxycinnamate in CCH-2 (0·5 wt %) (*a*) in the S_B phase at 35°C and (*b*) in the isotropic melt at 60°C, irradiation times are given in seconds.

cinnamates in smectic guest–host systems. Enhancements until the 400 fold of the values in isotropic melt were observed dependent upon the structure of cinnamates as well as on the smectic B solvent [32].

The efficiency of the cycloaddition was not affected by the nematic phase of CCH-4 or other nematic mesophases. Neither *E–Z* photoisomerization nor photocycloaddition were detected in a further smectic mesophase of CCH-4 in contrast to the photochemical behaviour in the other mesophases and isotropic melt of this liquid crystal.

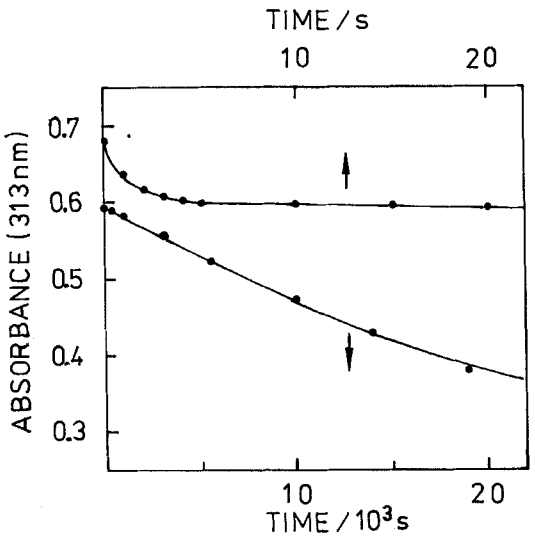

Figure 2. Absorbance at 313 nm in the photolysis of **1** at 60°C versus the irradiation time (the lines represent calculated curves).

Table 1. Relative quantum yield of (2+2) cycloaddition of 0·5 wt % *E*-ethyl 4-methoxycinnamate dissolved in CCH-2 and CCH-4 (λ_{exc} = 313 nm).

Matrix	T/°C	Mesophase	$\phi_{rel} \times 10^5$	r†
CCH-2	65	I	2·2	0·99
	32·5	S_B/N	12·0	0·99
	27	S_B/N	16·8	0·98
CCH-4	85	I	2·4	0·98
	75	N	1·4	0·99
	48	S_B/N	6·1	0·99
	38	S_2	0‡	—

† Correlation coefficients for the non-linear regression.
‡ Photodegradation does not take place in the time scale of the investigation.

2.2. *DSC and thermal polarizing microscopy*

The thermal properties of the pure liquid crystals as well as of the guest–host mixtures were estimated by DSC and thermal microscopy containing 0·5 or 5·0 wt % of **1** in CCH-2 and CCH-4. Figures 3 and 4 show textures of these samples with different guest concentrations and at different temperatures.

2.2.1. *CCH-2*

CCH-2 with 0·5 wt % has similar textures in all phases in comparison with the pure matrix. However, the N–I and S_B–N phase transitions are lowered and broadened for CCH-2 with 5 wt %. Thus, nematic droplets were observed at 46·9°C and a nematic schlieren texture was formed. The transition N to S_B was perceived at 38°C. As seen in figure 3 non-birefringent areas were formed in coexistence with a S_B texture below the bulk S_B–N transition temperature, which increase with decreasing temperature. These transitions are completely reversible.

(*a*) (*b*)

Figure 3. Photomicrographs of CCH-2 doped with **1**. (*a*) CCH-2 with 0·5 wt% at 33·4°C (S_B phase), (*b*) CCH-2 with 5 wt% at 33·8°C (microphase separated range).

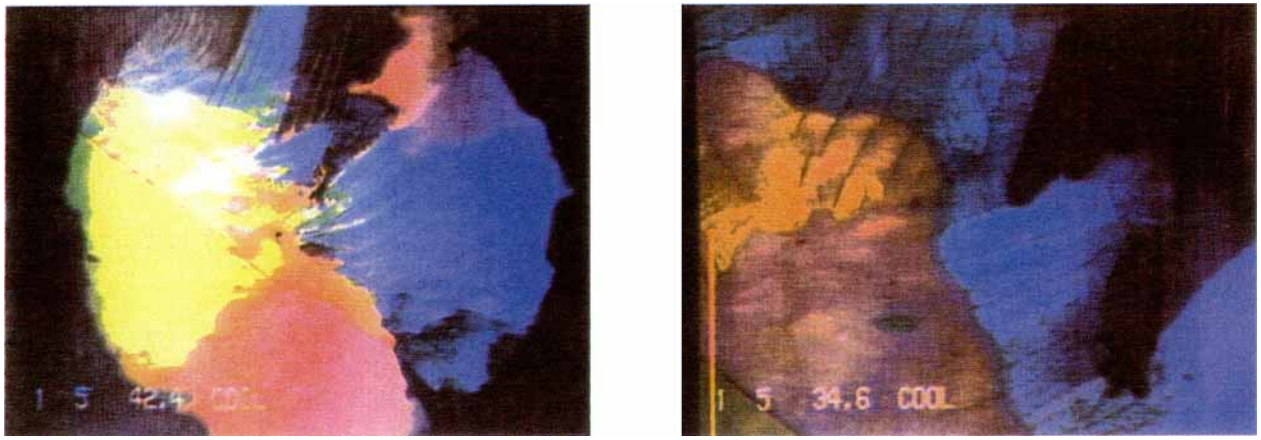

(*a*) (*b*)

Figure 4. Photomicrographs of CCH-4 doped with **1**. (*a*) CCH-4 with 0·5 wt% at 44°C (phase transition S_B to S_2), (*b*) CCH-4 with 0·5 wt% at 34·6°C (S_2 phase).

2.2.2. *CCH-4*

As seen in table 2, the N–I phase transition was lowered 1°C by 0·5 wt % of **1** and 4°C by 5·0 wt % of **1** and the S_B–N transition was lowered 2°C and 6°C, respectively. A two phase range of nematic and smectic areas was observed between 52°C and 45°C. A change of smectic B texture was found in the pure liquid crystal as well as in the guest–host mixtures at 46°C, lowering with increasing concentration. We interpret the texture as a new smectic mesophase between 46°C and 28°C. However, this phase transition was not detectable by DSC measurement. Thus, we suggest as phase sequence for CCH-4

$$C\ 28°C\ S_2\ 46°C\ S_B\ 54°C\ N\ 79°C\ I$$

The DSC thermograms of the sample with 0·5 wt % **1** show sharp transformation peaks for the other transitions, which are lowered and broadened with increasing concentration of the guest molecules. Transition temperatures obtained by different methods are summarized in table 2. Thus, the microscopic study makes the phase separation below the bulk S_B–N transition temperature clearly visible.

2.3. *NMR*

Providing a more complex characterization of photochromic guest–host mixtures the ^1H and ^{13}C NMR behaviour of CCH-2 and CCH-4 solvents as well as the ^2H NMR behaviour of solute cinnamate molecules have been investigated as a function of temperature and solute concentration.

Table 2. Transition temperatures of pure CCH-2 and CCH-4 as well as of the guest–host mixtures with **1**.

			Phase transition temperature		
Matrix	Addition of **1**	Method	T_{CS_B}/°C	T_{S_BN}/°C	T_{NI}/°C
CCH-2	0	Lit.	29	46	49
		DSC	—	46	53
		PM	(−13)	46	49
		^1H NMR	—	43	50
	0·5	DSC	—	48	54
		PM	(−13)	46	49
	1·0	^1H NMR	—	44	49
	5·0	DSC	—	43	52
		PM	(−15)	38	47
		^1H NMR	—	37	44
CCH-4	0	Lit.	28	54	79
		DSC	(2·5)	58	85
		PM	(5) *46†	54	79
		^1H NMR	—	54	80
	0·5	DSC	(5)	57	85
		PM	(5) *45†	52	78
	1·0	^1H NMR	—	52	78
	5·0	DSC	(4)	49	79
		PM	(4) *43†	48	75
		^1H NMR	—	48	73

† S_2-Phase.

Discussing the NMR results in mesophases we have to consider the relation between the observed line splitting or shift, the conformation of the molecule and the orientational order. In liquid-crystalline phases the fast anisotropic orientational motion leaves an averaged interaction tensor with an anisotropy different from zero. A line splitting $\Delta\nu_Q$ for quadrupolar interaction, line shift $\Delta\nu_c$ due to the chemical shift tensor or line broadening and splitting due to dipolar interaction determine the NMR spectra. In the simplest approximation we apply separate averaging of order fluctuations and intramolecular motions. Furthermore we only consider the orientational order parameter S assuming rod-like molecules. The deviation from axial symmetry is very small for longer molecules [40] and does not affect our main conclusions. Thus, we obtain for the quadrupolar interaction

$$\Delta\nu_Q = \tfrac{3}{2}\nu_Q\langle\tfrac{3}{2}\cos^2\beta - \tfrac{1}{2}\rangle(\tfrac{3}{2}\cos^2\tau - \tfrac{1}{2})S. \tag{1}$$

The quadrupole coupling constant ν_Q has a value of 170 kHz for the C–D bond, β is the angle between the C–D bond direction and the long molecular axis as shown in figure 5 and τ is the angle between the director and the magnetic field. The director for the bicyclohexyl-4-carbonitriles investigated oriented perpendicular to the applied magnetic field due to the negative diamagnetic anisotropy $\Delta\chi$ giving $-\frac{1}{2}$ for the last angular term in equation (1).

The two methylene deuterons of the solute are equivalent resulting in a single line pair in the spectrum. The fast hindered rotation of the CD_3 group averages the quadrupole coupling to $-\frac{1}{3}$ and the orientation parallel to the C–C rotation axis. Therefore, the ^2H spectrum consists of two pairs of lines with an intensity ratio of 2:3 and splittings [40]

$$\left.\begin{aligned}\Delta\nu_{Q_2} &= -\tfrac{3}{4}\nu_Q\langle\tfrac{3}{2}\cos^2\beta_2 - \tfrac{1}{2}\rangle S,\\ \Delta\nu_{Q_3} &= +\tfrac{1}{4}\nu_Q\langle\tfrac{3}{2}\cos^2\beta_c - \tfrac{1}{2}\rangle S.\end{aligned}\right\} \tag{2}$$

The ratio of the splittings is only dependent upon the conformation

$$v = \frac{\Delta\nu_{Q_2}}{\Delta\nu_{Q_3}} = \frac{-3\langle 3\cos^2\beta_2 - 1\rangle}{\langle 3\cos^2\beta_c - 1\rangle}. \tag{3}$$

A planar conformation with the long axis in the plane of the molecule and with idealized tetrahedral bonding angles could be assumed as a simple model as shown in figure 5. Then equation (2) can be expressed as a function of the angle ε formed between

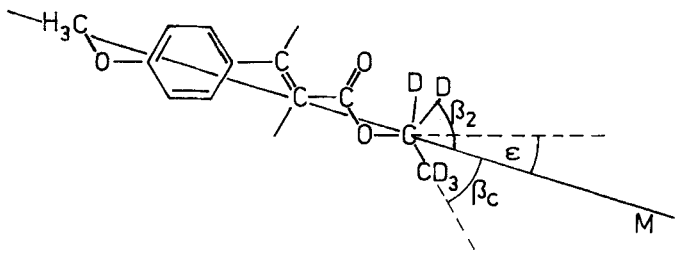

Figure 5. Postulated planar conformation of *E*-ethyl 4-methoxycinnamate.

the O–CD_2 direction and the molecular long axis M and the probability t and g for the *trans* and *gauche* state of the CD_3 group, respectively

$$\left.\begin{aligned}\Delta\nu_{Q_2} &= -63{\cdot}75\,\text{kHz}\frac{S}{1+2b}\{(1+b)[\cos^2(125{\cdot}3-\varepsilon)-1]+b[3\cos^2(70{\cdot}7-\varepsilon)-1]\},\\ \Delta\nu_{Q_3} &= +21{\cdot}75\,\text{kHz}\frac{S}{1+2b}\{3\cos^2(70-\varepsilon)-1+2b[\cos^2(125{\cdot}3-\varepsilon)-1]\}.\end{aligned}\right\} \quad (4)$$

Both values for *trans* and *gauche* are dependent upon the conformation energy, E_{tg}

$$t=\frac{1}{1+2b},\quad g=\frac{b}{1+2b}\quad\text{with}\quad b=\exp(-E_{tg}/k_BT). \quad (5)$$

In this way we obtained for the ratio of splitting equation (6)

$$v=\frac{3\{(1+b)(\sqrt{2}\sin\varepsilon-\cos\varepsilon)^2+b(\cos\varepsilon+2\sqrt{2}\sin\varepsilon)^2-3(1+2b)\}}{2b(\sqrt{2}\sin\varepsilon-\cos\varepsilon)^2+(\cos\varepsilon+2\sqrt{2}\sin\varepsilon)^2-3(1+2b)}. \quad (6)$$

The connection between v and ε is illustrated in figure 6 for $b=0$ (all *trans*) and $b=0{\cdot}2$ ($E_{tg}=4\,\text{kJ mol}^{-1}$). The sign of the experimentally determined ratio is unknown, but a negative sign was chosen since smaller values of ε are supposed. An increase of $|v|$ with decreasing temperature is then connected with larger ε as expected. The value of ε is used to deduce S according to equation (4). There may exist more conformations which should be taken into account, however, then the number of parameters increases significantly.

The high information content of ^{13}C NMR is based on the large chemical shifts δ_{iso} in the isotropic phase and on their tensor components (δ_1^a, δ_2^a, δ_3^a) in the oriented phases. With respect to the same assumption as for the deuteron splitting in equation (1) the line shifts of the different carbon positions i obey the relation

$$\Delta\nu_c=\nu_0[\delta_{iso}^i+\delta_{\zeta\zeta}S(\tfrac{3}{2}\cos^2\tau-\tfrac{1}{2})]. \quad (7)$$

In this case $\delta_{\zeta\zeta}$ is the component of the chemical shift tensor along the molecular axis. Our knowledge of the magnitude and orientation with respect to the shift tensors is not very precise.

The proton NMR line shape in liquid-crystalline phases is the result of intramolecular dipole interaction. A typical spectrum consists of a broadened triplet. The splitting of the outer lines is described by

$$\Delta\nu_0=S\Delta\nu_0\langle\tfrac{3}{2}\cos^2\beta-\tfrac{1}{2}\rangle(\tfrac{3}{2}\cos^2\tau-\tfrac{1}{2}), \quad (8)$$

where $\Delta\nu_0$ is the splitting of well separated proton pairs as present in the para-substituted phenyl rings. The CH_2 groups of the solvent molecules are not isolated and additional averaging due to internal motions and unfavourable angles β with the molecular axis provide an insufficient resolution. The experimentally observed line shape $g(\omega)$ is nearly independent of temperature and this fact justifies the simple scaling relation

$$g_S(\omega)=\frac{1}{S}g_1\left(\frac{\omega}{S}\right). \quad (9)$$

The second moment of the line used for further considerations then obeys

$$M_{2S}=S^2M_{20\perp}=S^2\tfrac{1}{4}M_{20\parallel}, \quad (10)$$

$M_{20\perp}$ and $M_{20\parallel}$ are the second moments for $S=1$ and for the magnetic field perpendicular and parallel to the director, respectively.

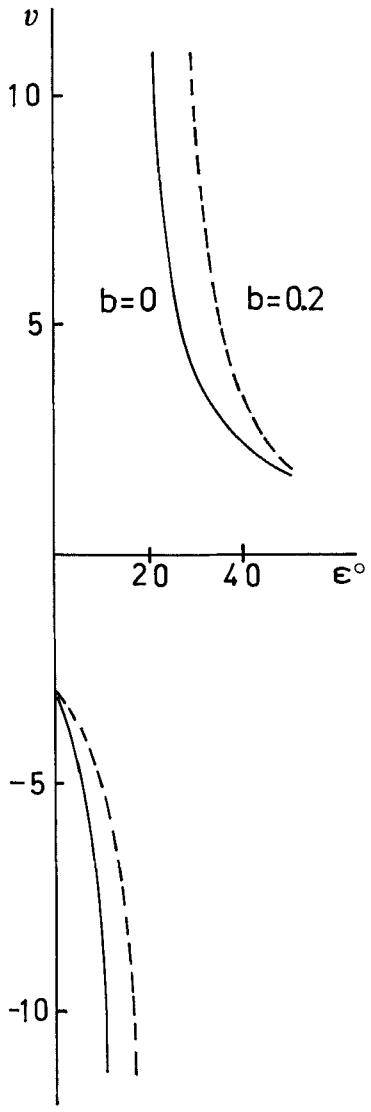

Figure 6. Connection between the ratio of quadrupole splitting v and the orientation of the long axis of the cinnamate molecule ε for tetrahedral bonding angles.

The proton line shape was drastically changed at the transition to the smectic B phase. Therefore, simple line shape calculations have been made starting with a good description of the nematic triplet structure, using

$$g(v)=I_S\left[\exp\left(\frac{-(v-F_0)^2}{2\Delta_s}\right)+\exp\left(\frac{-(v+F_0)^2}{2\Delta_s}\right)\right]+\exp\left(\frac{-v^2}{2\Delta_z}\right), \tag{11}$$

with appropriate values of Δ_s, Δ_z, where F_0 is the splitting of the outer lines, while Δ_s and Δ_z are gaussian broadening parameters. The calculated line shapes for spherical director distribution (powder) and a cylindrically symmetric distribution using the

same parameters are shown in figure 7. The relevant moments are $M_{2pow} = 0{\cdot}8\, M_{2S}$ and $M_{2cyl} = 1{\cdot}375\, M_{2S}$. The angular dependence of M_2 for a well oriented sample rotated around the axis perpendicular to the field is given by

$$M_2(\phi) = M_{2S}(\tfrac{27}{8}\sin^4\phi - 3\sin^2\phi + 1). \tag{12}$$

Some computations were carried out assuming rectangular or gaussian shape director distributions. Thus, figure 8 (*a*) demonstrates the variation in the line shape with the distribution parameter and figure 8 (*b*) shows that of M_2.

2.3.1. *^1H NMR of the solvents*

In figure 9 the temperature dependence of the line shape is shown for pure, 1·0 and 5·0 wt% cinnamate containing CCH-2 samples. The temperature dependence of the corresponding second moments is illustrated in figure 10 (*a*). The line shapes and the related M_2 values are similar for all samples in the nematic phase. The increase in M_2 values is caused by a growing orientational order with decreasing temperature, as described by equation (10). At the transition to the smectic B phase the line shape altered drastically and was also changed by the solute concentration. Thus, figure 10 (*a*) shows that the M_2 values are significantly dependent upon the solute concentration in the smectic B phase of CCH-2. Rotating the sample in the magnetic field the M_2 values were left unchanged. The gaussian line shape with the high second moment of 120 kHz^2 for the pure solvent could not be explained by a simple increase of the order parameter

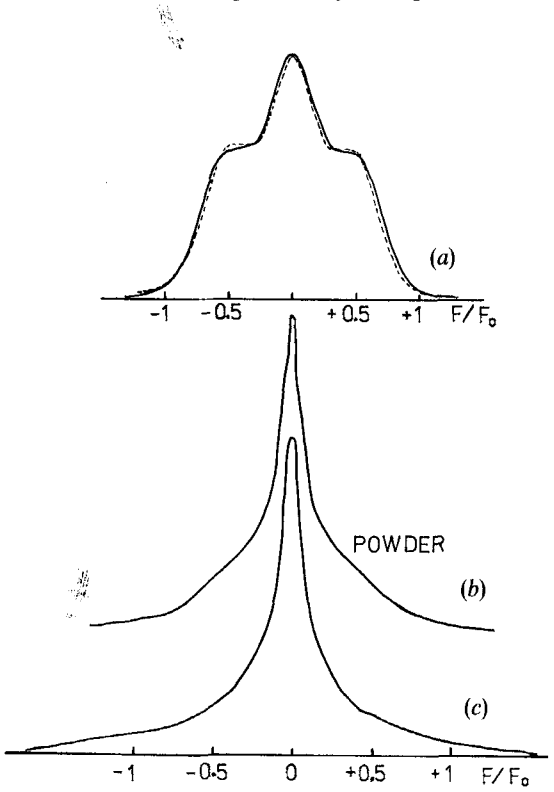

Figure 7. (*a*) Experimentally observed ^{1}H line shape (– –) and its theoretical approximation according to equation (11) (——) in the nematic phase. Calculated line shapes for spherical (*b*) and cylindrical (*c*) director distributions.

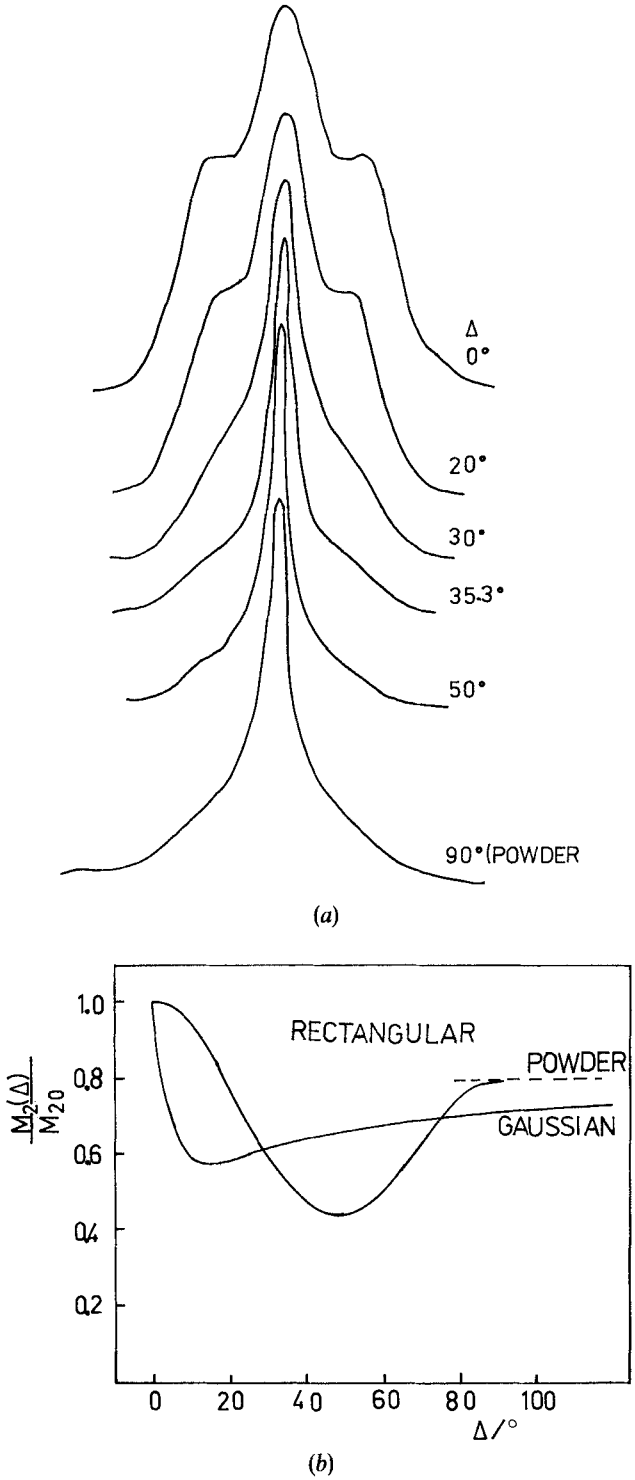

Figure 8. (*a*) Variation of the NMR line shape with increasing width Δ of the director distribution for a rectangular distribution function. (*b*) Corresponding change of M_2 for rectangular and gaussian functions.

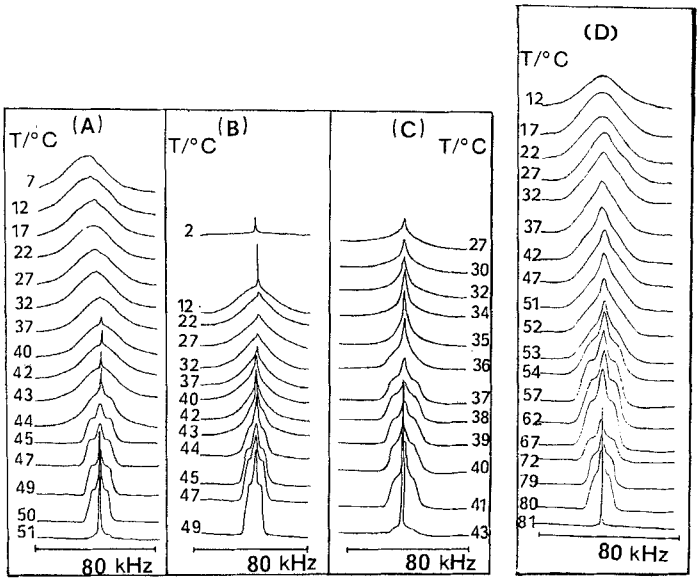

Figure 9. ^{1}H NMR line shape of CCH-2 and CCH-4 as a function of temperature and cinnamate concentration ((A) pure CCH-2, (B) 1·0 wt % in CCH-2, (C) 5·0 wt % in CCH-2, (D) pure CCH-4).

and a statistical director distribution, which gives the super lorentzian shape illustrated in figure 7. Therefore, we have to include a large contribution of intermolecular interactions to the M_2 values for the pure CCH-2 sample. This ought to be a consequence of a strong reduction of rotational and translational diffusion ($D \leqslant 10^{-14}\,m^2\,s^{-1}$ and $\tau_{rot} > 10^{-5}$ s). From the NMR point of view the behaviour of the CCH-2 molecules is more solid-like in the smectic B phase. However, the frequency of molecular tumbling increased in the mixtures probably due to a fast exchange between regular and distorted regions producing a change to a super lorentzian line shape.

Figures 9 (D) and 10 (*b*) show that CCH-4 exhibits a different NMR behaviour in comparison with CCH-2 concerning the temperature and the solute concentration dependence. The M_2 jumps of 10 kHz^2 at the phase transition T_{S_BN} were identical for pure and doped samples and much smaller than for CCH-2. The M_2 values increased with decreasing temperature within the smectic B phase. The M_2 value of a well oriented smectic phase with an order parameter S of 0·9 amounted to 69 kHz^2. The ratio M_{2exp}/M_{2theo} of 0·72 permitted the calculation of the director distribution width Δ. Thus, figure 8 yielded for the director distribution width $\Delta 4°$ or 110° for a gaussian distribution. The smaller value was supported by the observation of angular dependent line shapes or second moments (see figure 11). The variation obtained from the experiment, was restrained as expected for a director distribution. Comparison of the experimentally obtained ratio $M_2(0°)/M_2(90°)$ with theoretical curves calculated as a function of Δ also suggested a value of 2–4° for the distribution width of the director Δ.

2.3.2. ^{13}C *NMR of the solvents*

In figure 12 the aliphatic part of the ^{13}C NMR spectra of the CCH-2 molecules are shown in the isotropic melt, nematic and smectic phase. Similar spectra have also been observed for CCH-4. The different positions of the molecules were resolved in the

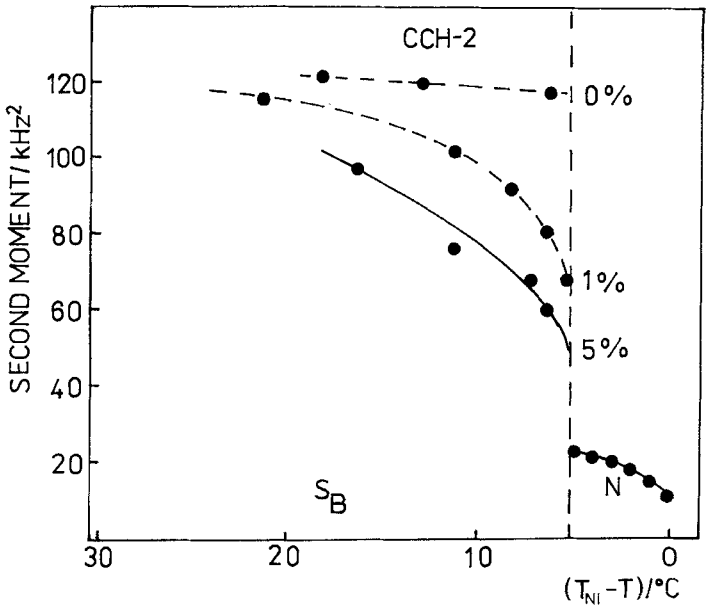

(*a*)

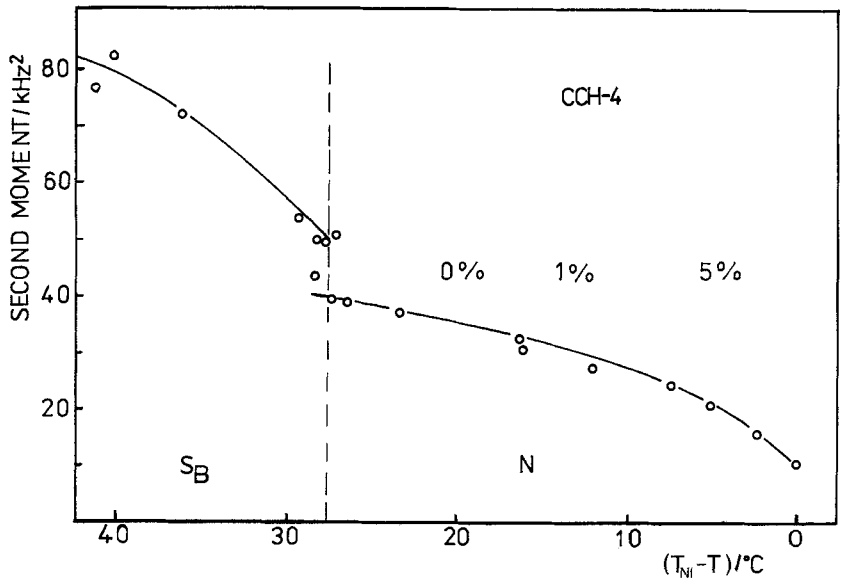

(*b*)

Figure 10. Temperature dependence of the second moments at various cinnamate concentrations (normalized to the clearing temperature T_{NI}), (*a*) CCH-2, (*b*) CCH-4.

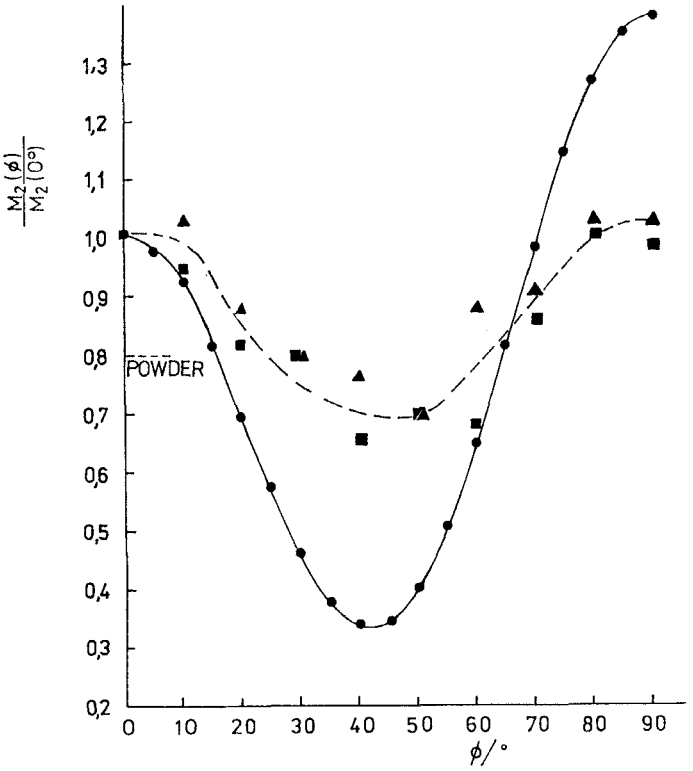

Figure 11. Angular dependence of the observed M_2 values for CCH-4 in comparison to the theoretical curve (●). Experimental values for CCH-4 with 5·0 wt% at 310 K (■) and 305 K (▲).

nematic phase, however the line shifts were too small to use the values for the calculation of the order parameter ($\delta \leqslant 5$ ppm). The cyanoline was shifted more strongly (about 40 ppm) in the nematic phase. The intensity of the cyanoline related to the other lines decreased in the nematic phase nearly by a factor of ten, probably due to the CN dipolar interaction. Using $\delta_{\zeta\zeta} = -200$ ppm the order parameter S was deduced from the line shift according to equation (7). For the concentrated CCH-4 sample also strong aromatic lines of the solute have been detected and used for the calculation of S. The smectic B phase of CCH-2 obtained were not oriented as can be seen from the powder-like spectra in figure 12. The width of the lines is given by the shift anisotropy and therefore larger for the chain positions.

As already mentioned the smectic B phase of CCH-4 is better oriented giving resolved lines for a few positions with 25 per cent higher shift value (and order parameter). Simultaneously typical lines with decreasing intensity could be detected up to 8 K below the S_B–N transition. Despite the low intensity the well-isolated line of the CN group was used to deduce the relative amount of the CCH solvent molecules in the nematic state.

2.3.3. ^2H *NMR spectra of E-ethyl 4-methoxycinnamate*

The solvent dependent behaviour of dissolved cinnamate molecules has been investigated by their ^2H spectral pattern. The spectra consisted of an inner pair of lines with a higher intensity from the CD_3 group and the outer pair from the CD_2 moiety.

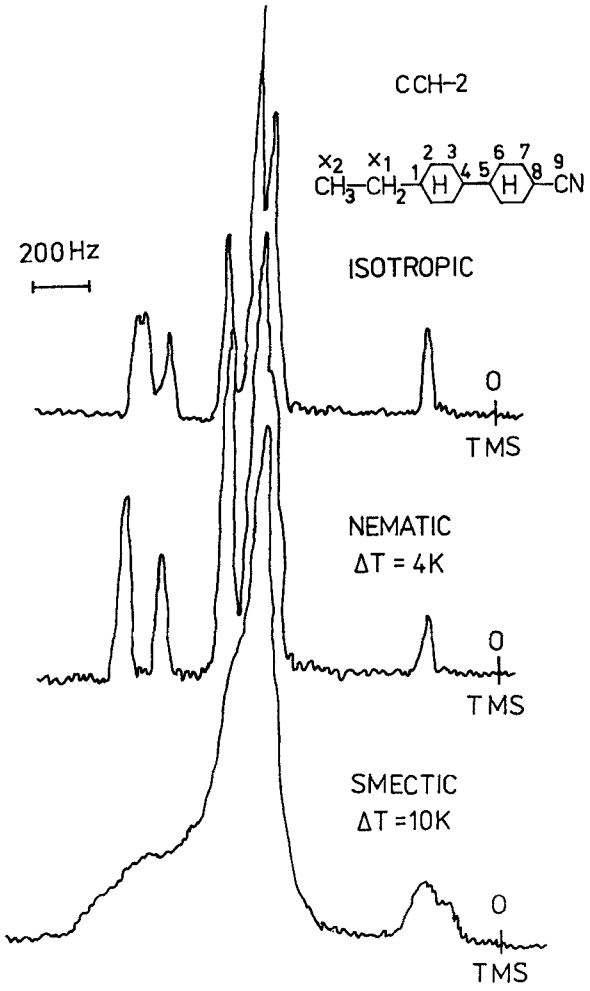

Figure 12. ^{13}C NMR spectra of CCH-2, the frequency range of 60 ppm contains only the aliphatic carbons.

Figure 13 shows the temperature dependence of the quadrupole splittings normalized to the clearing temperatures for 1·0 wt % and 5·0 wt % solute concentration in CCH-2. The influence of the solute concentration was very small. The increase in splitting within the nematic phase was caused by the growing order parameter S. However, the splitting decreased at the transition to the smectic phase and within the smectic B phase with decreasing temperature. But the line shape and width of solute spectra remained unchanged.

The experimentally observed ratio of the two quadrupole splittings was 11·2 and was nearly independent of temperature and liquid crystal phase. An ε value of $17{\cdot}5 \pm 0{\cdot}2°$ was obtained using equation (5) with $b = 0{\cdot}2$ and the negative sign of v (see figure 6). Using this ε the order parameter of the solute could be evaluated without further assumptions according to equation (4). The temperature dependence of the order parameter for the guest molecules as well as for the CCH solvents is shown in

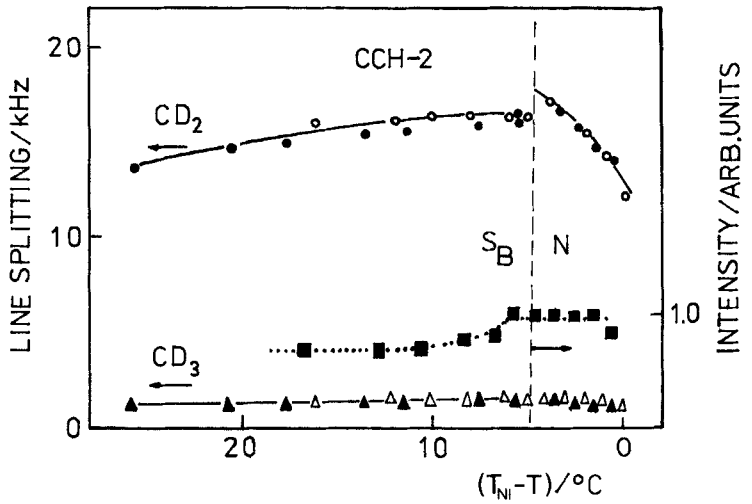

Figure 13. Quadrupole splitting $\Delta\nu_Q$ (● ▲ 1·0 wt % and ○ △ 5·0 wt % of **1**) and intensity i (■) of 1·0 wt % cinnamate dissolved in CCH-2, temperature normalized to the clearing temperature T_{NI}.

figure 14. The order parameter of the CCH-2 solvent was determined using a value of the second moment $M_{20\perp} = 90\,\text{kHz}^2$. The order parameter of the guest molecules is lower in the nematic phase than that of the solvent molecules, but the same temperature dependence was observed. The sharpness of the ^{2}H lines is unchanged at the transition to the smectic phase. The intensity decreased only a few per cent for the 1·0 per cent sample as shown in figure 13. Rotating the sample by 90° left the splitting unchanged, but the intensity decreased slightly. These facts allow us to conclude that guest molecules are dissolved in nematic surroundings below the bulk smectic B–nematic transition, whereas the majority of the solvent molecules form a smectic B phase according to the ^{1}H and ^{13}C NMR results. The dimension of the nematic regions is large enough to be oriented by an external magnetic field (diameter greater than 1·0 μm). The nearly constant intensity of the ^{2}H spectra above and below the phase transition S_B–N indicates that most of the cinnamate guest molecules (90 per cent in the sample with a total concentration of 1·0 per cent cinnamate) were solubilized in a nematic phase. Lowering the temperature the decreasing intensity of the CN line in the ^{13}C NMR spectra reflects the reduced portion of solvent molecules in the nematic state. The increasing concentration of the non-mesogenic cinnamate caused a decrease of order parameter of the solute in this state.

On further cooling to 24°C the quadrupole splitting disappeared abruptly and a single isotropic line was observed. The distortion of the nematic surroundings due to the high concentration of the non-mesogenic cinnamate molecules was so strong that an isotropic phase was formed. However, the solvent was still arranged in a super cooled smectic B phase.

The ^{2}H spectra of the cinnamate **1** in CCH-4 corresponded to the spectra of **1** in the CCH-2 mixture, but they deviated in a few important details, as seen in figure 15. The splitting increased in the nematic phase as a result of growing order. Within the large nematic temperature range the ratio of the two splittings varied from $-10{\cdot}6$ to -12 which corresponds to an increase in the tilt angle ε from 17·1 to 18·1°, according to

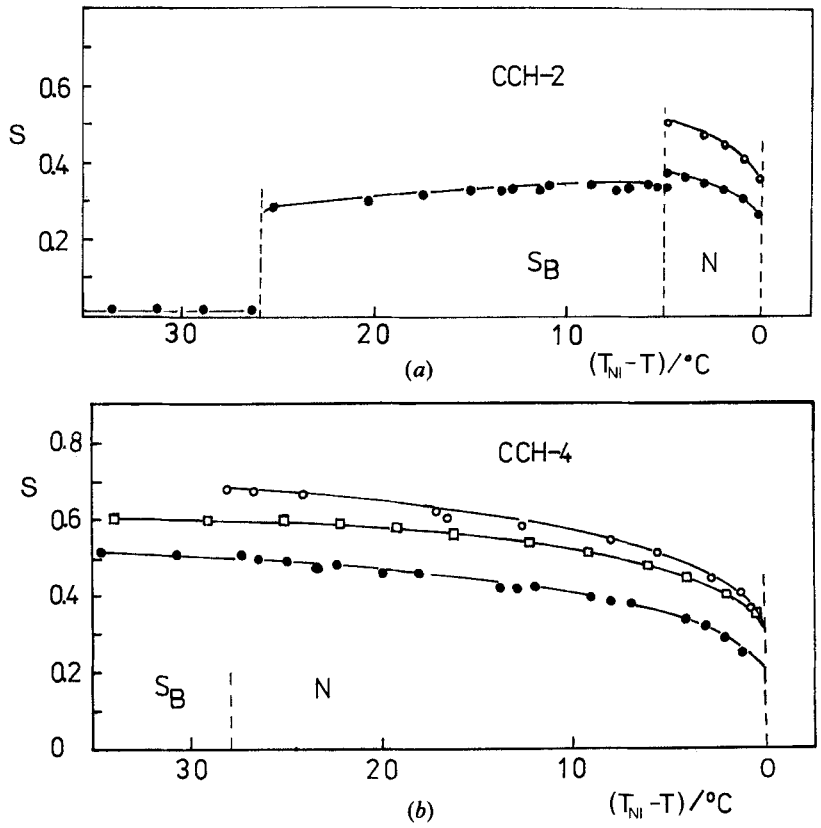

Figure 14. Order parameter S of the *E*-ethyl 4-methoxycinnamate in CCH-2 and CCH-4 (●) (^{2}H NMR) and order parameter S of CCH-2 and CCH-4 matrix by ^{1}H NMR (○) and ^{13}C NMR with 5·0 wt% of **1** (□) as a function of temperature (normalized to the clearing temperature T_{NI}) in mixtures with 1·0 wt% cinnamate **1**.

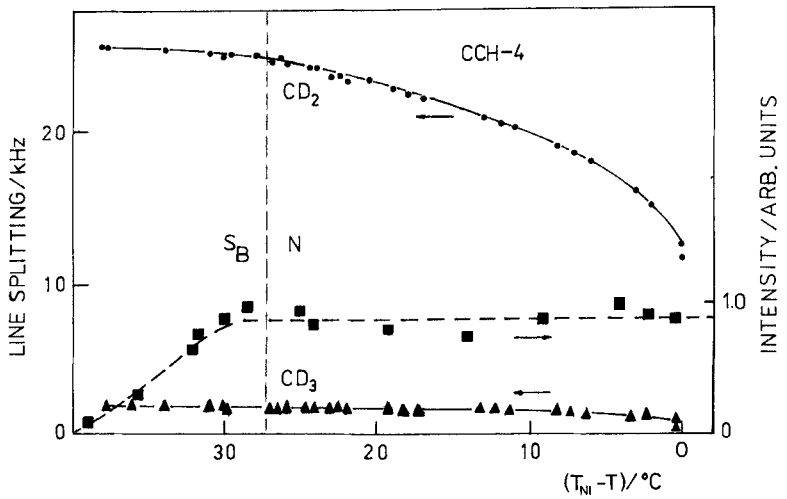

Figure 15. Quadrupole splitting $\nu\Delta_Q$ and intensity i (■) of cinnamate (1·0 and 5·0 wt%) dissolved in CCH-4, temperature normalized to the clearing temperature T_{NI}.

equation (6). This should be expected, if the *trans* conformation attains a higher probability. The order parameter given in figure 14 (*b*) was calculated using a constant mean value of ε for the solute and $M_{20\perp} = 84\,\mathrm{kHz}^2$ for the solvent. The values for the order parameter in the nematic phases of CCH-4 and CCH-2 were in good agreement. However, the phase transition S_B–N in CCH-4 solvent did not exert any influence on the quadrupole splitting and linewidth in contrast to the behaviour in the CCH-2 mixtures. Referring to the same arguments as discussed previously the detected cinnamate molecules are dissolved in nematic regions of the biphasic mixture. The solute molecules incorporated into the smectic surroundings could not be observed due to the large linewidth. On cooling the intensity dropped continuously to zero within a temperature range of 10°C in the smectic B phase. In this range approximately 70 per cent of the cinnamate molecules were arranged in the nematic areas of the biphasic mixture. However, on further cooling cinnamate molecules were incorporated into the smectic lattice. In contrast to CCH-2 the order parameter of the solute changed continuously to higher values. The formation of isotropic regions could not be observed for 1·0 per cent of the solute or only with low intensity a few degrees above the crystallization point.

The results deduced from the ^{13}C NMR confirmed these conclusions. The S values of the solvent agreed quite well with the proton results, only near the smectic B phase was a stronger saturation (lower S) observed. Conformational changes supported by the variation of v and also by small changes in the ratio of carbon shifts may additionally increase the M_2 values.

The aromatic lines on the solute are shifted opposite to the CN line, that means $\delta^{\mathbf{A}}_{\xi\xi} > 0$ as expected and an orientation of the long molecular axis parallel to the director occurred. The $\delta_{\xi\xi}$ values required to obtain the order parameter from the ^{2}H spectrum were unexpectedly high.

3. Discussion

The starting point for the investigation was the surprisingly high quantum yield of (2 + 2) photocycloaddition in ordered and highly viscous smectic B phases of several liquid crystals compared to the reaction in nematic phases or isotropic melts. Thus, the guest–host interaction of deuteriated *E*-ethyl 4-methoxycinnamate has been studied in liquid-crystalline solutions of CCH-2 and CCH-4 by DSC, thermal microscopy, ^{2}H NMR of the solute as well as ^{13}C NMR and ^{1}H NMR of the solvent. Obviously, there are distinctions between characterizing the guest–host mixtures by different methods and the situation of the photochemical experiments. Thus, cinnamate molecules in the excited state have properties different to the molecules in its ground state. Moreover, on irradiation a large amount of *E*-cinnamate molecules is converted to the *Z* isomer owing to photoisomerization. This isomer has a modified geometrical shape and a different dipole moment. The solubilization of cinnamate and the order of the guest–host system may be influenced to a certain extent hitherto unknown compared to the investigation of solubilization of *E*-cinnamate in the ground state.

In most photochemical and spectroscopic investigations using mesogenic solvents only the behaviour of the solute was observed with regard to order, dynamics and photoreactivity. However, a better understanding can be obtained by more complex studies including the matrix of the real guest–host system as well as the photochromic guest molecules. Incorporation of a solute in a liquid-crystalline matrix results in a certain degree of disruption of the solvent order in the surroundings of the solute and orientation of guest molecules. Our results give an interpretation for the phase and

temperature dependence of the solubilization behaviour and of (2+2) photocycloaddition of a rod-like, but non-mesomorphic cinnamate in solutions of CCH-2 and CCH-4.

The investigation has proved by experience that the solubility of this non-mesogenic molecule can be high in the nematic phases. However, the cinnamate **1** has a very low solubility in the smectic B phase of these liquid crystals. The lattice-like structures are more sensitive to heterogeneous molecules which disturb the regular arrangement within the smectic layers. Thus, the results suggest that cinnamate **1** has a maximum solubility much less than 0·5 wt% in the smectic B phase of CCH-2 but somewhat higher in CCH-4. Higher concentrations of solute **1** cause phase separation solubilizing cinnamate molecules in nematic or isotropic phases depending on concentration and temperature as well as the structural requirements of solvent and solute.

The guest molecules reside both in smectic B matrix and in microphase separated nematic or isotropic areas, which coexist with the smectic B phase. Thus, the portion and the composition of the nematic phase of guest–host mixtures have been estimated dependent upon the temperature. The portions of cinnamate and CCH solvent molecules within the nematic phase are summarized with regard to total concentration in table 3. The portion of cinnamate, which has been solubilized in the pure or phase separated nematic phase has been estimated by the line intensity of ^{2}H NMR spectra with a total concentration of 1·0 wt% cinnamate, as shown in figures 13 and 15. The content of the solvent molecules within the phase separated nematic volume has been calculated by ^{13}C NMR for 3·0 wt% cinnamate mixtures.

Table 3. Portion of cinnamate and CCH-*n* molecules in the nematic phase in relation to the total amount of solute or solvent molecules as a function of temperature.

			Portion in nematic state	
Matrix	*T*/°C	Phase†	CCH-*n*‡	Cinnamate§
CCH-2	42	N	1·00	1·0
	40	N	1·00	
	38	S_B/N	0·78	0·9
	37	S_B/N	0·82	
	33	S_B/N	0·58	
	32·5	S_B/N	0·42	
	32	S_B/N	0·38	0·9
	29	S_B/N	0·28	
	25	S_B/N	0·20	
	24	S_B/I	0	0
CCH-4	59	N	1·00	1·0
	46	S_B/N	0·71	0·74
	41	S_2	0·50	
	37	S_2	0·37	0·2
	36	S_2	0·27	
	32	S_2	0·21	
	28	S_2	0·21	

† S_B/N–biphasic smectic B/nematic.
‡ With 3 wt% of **1** using ^{13}C NMR (the intensity of the CN line with an error of 30 per cent).
§ With 1 wt% of **1** using ^{2}H NMR.

In the CCH-2 mixtures with 0·5, 1·0 and 5·0 wt % of **1** the cinnamate molecules are dissolved nearly completely in the nematic regions of the biphasic system, as shown in table 3. The composition of this nematic phase changes continuously to higher concentrations of cinnamates with decreasing temperature by incorporating further CCH-2 molecules into the S_B lattice. In this way, the solute order parameter of **1** appears to decrease with lowering the temperature below the bulk S_B–N transition temperature for CCH-2, as shown in figure 14. On continued cooling the minor, cinnamate-rich nematic component of the two phase system transforms into an isotropic liquid at 24°C. The formation of a smectic B–isotropic biphasic system was observed. The transformation to a plastic crystal as proposed previously [6, 12, 22, 23] can be excluded [4].

This heterogeneous solubilization or phase separation causes a compartmentalization of the cinnamates in solute-rich nematic or isotropic phases below the bulk S_B–N transition temperature. The enriched concentration of **1** in these phase separated volumes should be the principal reason for the higher quantum yield.

Table 3 indicates that roughly 42 per cent of CCH-2 molecules and 90 per cent of the cinnamate molecules form the nematic phase at 32·5°C. Thus, the local concentration of the photoreactive solute is approximately two times larger and the quantum yield obtained was 5·4 times larger compared to the corresponding value of the homogeneous isotropic melt. This enhancement is in agreement with the kinetic law for bimolecular reactions.

In the CCH-4 solvent the cinnamate molecules are partly incorporated in the smectic hexagonally ordered layers and the other part (only 74 per cent at 46°C) is dissolved in nematic regions of the biphasic S_B–N state existing within the first 7°C below the phase transition (see figure 15). However, the compartmentalization effect seems to be smaller than in CCH-2. The amount of cinnamate molecules in the nematic phase decreases systematically with decreasing temperature until 7°C below T_{S_BN} (see table 2). At this temperature a phase transition to another smectic phase was observed. This phase transition was also detected by means of ^{13}C NMR spectroscopy and proton T_1 measurements. The relaxation of CCH-4 molecules is drastically restricted below this temperature. There is not any structural evidence for the kind of phase by X-ray diffraction until now.

Concerning CCH-2 the phase separation occurs throughout the temperature range of the smectic B phase. For CCH-4 an increasing part of the solute molecules was incorporated into the lattice especially in the new S_2 phase. Thus, a nearly complete solubilization of the cinnamate occurs in this smectic phase. The concentration of the solute in the nematic part of the matrix remains approximately constant leading to the observed continuous increase of S and explaining the absence of an isotropic phase at low temperatures.

The quantum yield of cycloaddition is also high in the microphase separated regions of the CCH-4. However, neither *E*–*Z* photoisomerization nor (2 + 2) photocycloaddition were observed for this guest–host system of **1** in the second smectic phase of CCH-4. This smectic matrix causes a restriction of conformational mobility and translational diffusion of dissolved and isolated cinnamate molecules.

The matrix dependence of the *E*–*Z* photoisomerization allows us to conclude that the solvent order of the smectic phases can impart a very dramatic inhibitory effect on the conformational mobility of the excited state of the dissolved solutes. Thus, the *E*–*Z* isomerization is restricted completely in the second smectic phase of CCH-4, where 90 per cent of the cinnamate molecules are incorporated into this lattice. The reaction is inhibited partially in the biphasic S_B/N or S_B/I composition of CCH-2. This fact

suggests that the molecules undergo isomerization in the nematic and isotropic phases. However, the fraction of cinnamate solubilized in the smectic B phase is not capable of reacting under these conditions. The results demonstrate that unimolecular reactions may be restricted by highly ordered smectics due to a restraint on the molecular geometry of the solute in the excited state or of the photoproducts.

In ordered systems bimolecular reactions may be promoted or inhibited depending on the relative orientation of the reactive molecules, reaction coordinate and motional anisotropy of the substrate. Generally, enhancement of the rate or quantum yield is expected, when a favourable reactant orientation of colliding molecules or ground state aggregation which prefigure the transition state are driven by an anisotropic solvent. Such orientational effects are expected to act on the entropic part of the reaction free energy of activation. Weiss has suggested that photodimerization of acenaphthylene is enhanced by controlling the collision orientation of the excited molecule and a second ground state molecule by the specific orientation and the anisotropy of diffusion. Moreover, the stereoselectivity of the (2 + 2) photocycloaddition of cinnamates has been interpreted by preferred ground state head-to-tail aggregation. The combination of dipole–dipole interaction of cinnamates and the orientational order of mesophases should yield pairwise, antiparallel, interdigitated alignment of cinnamate molecules [21].

Recently, Samori has proposed heterogeneous solubilization effects within the spheres of rigid cores or less ordered chains of smectic B phases [4]. This solute distribution among different solubilization sites causes different reactive sites of a thermal bimolecular reaction. However, our results, especially the continuous behaviour of the ^2H line splitting and its ratio, demonstrate that the observed increased quantum yield of cycloaddition is not caused by reactive sites on a molecular level, but compartmentalization occurs by phase separation. Based on our results we conclude that the solvent-induced concentration effect (compartmentalization) is the dominant factor for the enhancement of the quantum yield in this guest–host system. However, the contribution of solvent-induced orientational effects cannot be excluded in the cinnamate-rich nematic component of this biphasic system. The topic of a further publication will be the enhancement of the photocycloaddition of different substituted cinnamates with a wide variation in geometrical shape and electric dipole moments in the smectic B phases of several liquid crystals [32]. The experiments suggest that both solvent induced orientation and concentration effects have to be discussed for interpretation.

It is amazing that such large differences exist between similar molecules as CCH-2 and CCH-4 as host matrices with respect to solubilization and photoreactivity of cinnamate. CCH-2 is more sensitive to heterogeneous guest molecules, which is demonstrated by the concentration dependence of the second moments, as seen in figure 10 (*a*). The polar molecules of some CCH-*n* derivatives, such as CCH-3, CCH-4 and CCH-5, are arranged in head-to-tail orientation and form a bilayer structure of the smectic B phase with interdigitation of alkyl groups and cyano moieties. However, there are differences between several CCH-*n* in miscibility [5, 37] and order [5, 8, 41, 42]. Thus, CCH-4 forms a hexagonally ordered smectic phase with two molecules in the unit cell [36], which is similar to that of CCH-3 but with a higher order. In contrast to that CCH-2 shows a rhombohedral structure, the order of which is even higher than that of CCH-4 [5, 8]. The lattice and/or the short alkyl chains compensate insufficiently disruptions and cause a smaller miscibility of the disordered regions surrounding the cinnamate molecules.

The *E–Z* photoisomerization indicates the restriction of conformational mobility. The efficiency of the bimolecular photocycloaddition indicates the distribution of reactive site geometries and concentrations in these solvents. In this way, the photoreactions may be said to act as a proof of the micromorphology of liquid crystals. Various studies and reported effects of liquid-crystalline solvents, essentially of smectic B phases, on bimolecular reaction have to be critically examined with regard to these results.

References

[1] KALYANASUNDARAM, K., 1987, *Photochemistry in Microheterogeneous Systems* (Academic).
[2] RAMAMURTHY, V., 1986, *Tetrahedron*, **42,** 5753.
[3] STUMPE, J., and KREYSIG, D., 1990, *Selected Topics in Liquid Crystal Research*, edited by H. D. Koswig (Akademie Verlag).
[4] SAMORI, B., 1988, *Polarized Spectroscopy of Ordered Systems*, edited by B. Samori and E. W. Thulstrup (Kluwer).
[5] ZIMMERMANN, R. G., LIU, J. H., and WEISS, R. G., 1986, *J. Am. chem. Soc.*, **108,** 5264.
[6] NERBONNE, J. M., and WEISS, R. G., 1979, *Israel. J. Chem.*, **18,** 266.
[7] LEIGH, W., 1985, *J. Am. Soc.*, **107,** 6114.
[8] LEIGH, W., 1986, *Can. J. Chem.*, **64,** 1130.
[9] TREANOR, R. L., and WEISS, R. G., 1986, *J. Am. chem. Soc.*, **108,** 3137.
[10] HROVAT, D. A., LIU, J. H., TURRO, N. J., and WEISS, R. G., 1984, *J. Am. chem. Soc.*, **106,** 7033.
[11] TRENOR, R. J., and WEISS, R. G., 1987, *J. Phys. Chem.*, **91,** 5552.
[12] FAHIE, B. J., MITCHELL, D. S., WORKENTIN, M. S., and LEIGH, W. J., 1989, *J. Am. chem. Soc.*, **111,** 2916.
[13] AVIV, G., SAGIV, J., and YOGEV, A., 1976, *Molec. Crystals liq. Crystals*, **36,** 349.
[14] KUNIEDA, T., TAKAHASHI, T., and HIROBE, M., 1983, *Tetrahedron Lett.*, **24,** 5107.
[15] NERBONNE, J. M., and WEISS, R. G., 1978, *J. Am. chem. Soc.*, **100,** 2571.
[16] NERBONNE, J. M., and WEISS, R. G., 1979, *J. Am. chem. Soc.*, **101,** 402.
[17] NAKANO, T., and HIRATA, H., 1982, *Bull. chem. Soc. Jap.*, **55,** 947.
[18] TANAKA, Y., and TSUCHIYA, H., 1979, *J. Phys., Paris*, **40,** C3–41.
[19] TANAKA, Y., TSUCHIYA, H., SUZUKI, M., and TSUDA, K., 1981, *Molec. Crystals liq. Crystals*, **68,** 133.
[20] RAMESH, V., and WEISS, R. G., 1986, *Molec. Crystals liq. Crystals*, **135,** 13.
[21] RAMESH, V., and WEISS, R. G., 1986, *J. org. Chem.*, **51,** 2535.
[22] LIN, Y., and WEISS, R. G., 1989, *Liq. Crystals*, **4,** 367.
[23] SISIDO, M., TAKEUCHI, K., and IMANISHI, Y., 1984, *J. Phys. Chem.*, **88,** 2893.
[24] ANDERSON, V. C., CRAIG, B. B., and WEISS, R. G., 1981, *J. Am. chem. Soc.*, **103,** 7169.
[25] ANDERSON, V. C., CRAIG, B. B., and WEISS, R. G., 1982, *J. Am. chem. Soc.*, **104,** 2972.
[26] ANDERSON, V. C., CRAIG, B. B., and WEISS, R. G., 1982, *J. Phys. Chem.*, **86,** 4642.
[27] STUMPE, J., SELBMANN, CH., and KREYSIG, D., 1991, *J. Photochem. Photobiol.* A, **58,** 15.
[28] HROVAT, D. A., LIU, J. H., TURRO, N. J., and WEISS, R. G., 1984, *J. Am. chem. Soc.*, **106,** 5291.
[29] HENTZE, F., and PELZL, G., 1977, *Z. Chem.*, **17,** 294.
[30] RENNERT, J., 1971, *Photogr. Sci. Eng.*, **15,** 60.
[31] STOBBE, H., and STEINBERGER, F. K., 1922, *Ber.* B, **55,** 2225.
[32] STUMPE, J., WOLF, K., and KREYSIG, D., *Molec. Crystals liq. Crystals* (submitted).
[33] WEDEL, H., and HAASE, W., 1978, *Chem. Phys. Lett.*, **55,** 96.
[34] JEDE, F., STRATEMANN, A. W., and SCHRADER, B., 1986, *Molec. Crystals, liq. Crystals*, **40,** 297.
[35] FUNG, B. M., and GANGODA, M., 1985, *J. Am. chem. Soc.*, **107,** 3395.
[36] RAHIMZADEH, E., TSANG, T., and YIN, L., 1986, *Molec. Crystals, liq. Crystals*, **139,** 291.
[37] MICHELL, D. S., and LEIGH, W. J., 1989, *Liq. Crystals*, **4,** 39.
[38] TAKAHASHI, K., 1987, *Molec. Crystals, liq. Crystals* (b), **150,** 387.
[39] SCHWETLICK, K. (editor), 1986, *Autorenkollektiv 'Organikum'* (VEB Deutscher Verlag der Wissenschaften, Berlin).
[40] GRANDE, S., LIMMER, ST., SCHMIEDEL, H., and STANARIUS, R., 1990, *Selected Topics in Liquid Crystal Research*, edited by H. D. Koswig (Berlin: Akademie Verlag).
[41] BROWNSEY, G. J., and LEADBETTER, A. J., 1981, *J. Phys. Lett., Paris*, **42,** 135.
[42] HAASE, W., and PAULUS, H., 1983, *Molec. Crystals liq. Crystals*, **100,** 111.
[43] WEISS, R. G., 1988, *Tetrahedron*, **44,** 3413.